Anal. Chem. **2000,** *72,* 5994−6002

Subsecond Adsorption and Desorption of Dopamine at Carbon-Fiber Microelectrodes

Bradley D. Bath, Darren J. Michael, B. Jill Trafton, Joshua D. Joseph, Petrise L. Runnels, and R. Mark Wightman*

Department of Chemistry, University of North Carolina at Chapel Hill, Chapel Hill, NC 27599-3290

High-repetition fast-scan cyclic voltammetry and chronoamperometry were used to quantify and characterize the kinetics of dopamine and dopamine-*o*-quinone adsorption and desorption at carbon-fiber microelectrodes. A flow injection analysis system was used for the precise introduction and removal of a bolus of electroactive substance on a sub-second time scale to the disk-shaped surface of a microelectrode that was fabricated from a single carbon fiber (Thornel type T650 or P55). Pretreatment of the electrode surfaces consisted of soaking them in purified isopropyl alcohol for a minimum of 10 min, which resulted in S/N increasing by 200−400% for dopamine above that for those that were soaked in reagent grade solvent. Because of adsorption, high scan rates (2000 V/s) are shown to exhibit equivalent S/N ratios as compared to slower, more traditional scan rates. In addition, the steady-state response to a concentration bolus is shown to occur more rapidly when cyclic voltammetric scans are repeated at short intervals (4 ms). The new methodologies allow for more accurate determinations of the kinetics of neurotransmitter release events (10−500 ms) in biological systems. Brain slice and in vivo experiments using T650 cylinder microelectrodes show that voltammetrically measured uptake kinetics in the caudate are faster using 2000 V/s and 240 Hz measurements, as compared to 300 V/s and 10 Hz.

The adsorption properties of carbon-based materials have been well-recognized for many years. For example, water purification systems take advantage of carbon's adsorptive characteristics to remove both organics and chlorine. Carbon can also be used to purify reagent grade organic solvents, such as 2-propanol. Here, highly porous or activated carbon adsorbs unwanted organic contaminants, providing a facile technique for purification.[1] In the electrochemical measurements described herein, adsorption processes at carbon-fiber electrodes are shown to be of importance in the analysis of catecholamines and in the evaluation of the temporal response of the overall signal.

The process of adsorption and its influence on double-layer structure is quite well-understood at mercury electrodes.[2] Thermodynamic models can be used to describe adsorption/desorption phenomena.[3] In addition, studies modeling the kinetics of adsorption have also been undertaken. These models describe adsorption kinetics that are fast in comparison to diffusion of the adsorbate to the electrode surface.[4] In the present report, adsorption/desorption kinetics of the catecholamine, dopamine (DA), are probed under conditions in which mass transport is not rate-limiting. A microelectrode is positioned at the outlet of a flow injection apparatus and is exposed to a bolus of a known concentration of DA. Exposure times are short (0.5−2 s) and the dynamics of the electrochemical response are solely affected by the adsorption and desorption kinetics of DA and its oxidized form, dopamine-*o*-quinone (DOQ).

Two types of carbon fibers have been investigated. Thornel P55 fibers are manufactured from a pitch precursor. Thornel T650 fibers are made from polyacrylonitrile. The differences lead to subtle changes in surface chemistry. In addition, P55 fibers are larger, ∼10-μm diameter, in comparison to T650s, ∼7-μm diameter. Both types have been widely used in microelectrodes to investigate neurotransmission events in biological matrixes.[5]

Many studies aimed at understanding catecholamine and quinone electrochemistry have been performed, due to their great importance in biological systems.[6] DA is a neurotransmitter that is released at the synaptic cleft between two neurons and is found in many discrete regions throughout the central nervous system. DA neurotransmission has been related to a variety of behaviors including reward mechanisms in the brain and motivational habit.[7] For example, consumption of amphetamine or cocaine has been shown to lead to elevated levels of DA in the brain for extended periods of time.[8] In vivo electrochemical procedures are ideally suited for the measurement of several physiological parameters,

* Corresponding author. E-mail: rmw@unc.edu.

(1) Ranganathan, S.; Kuo, T. C.; McCreery, R. L. *Anal. Chem.* **1999**, *71*, 3574−3580.

(2) Bard, A. J.; Faulkner, L. R. *Electrochemical Methods*; John Wiley and Sons: New York, 1980; pp 488−552.

(3) (a) Delahay, P.; Mohilner, D. M. *J. Am. Chem. Soc.* **1962**, *84*, 4247−4252. (b) Woopschall, R. H.; Shain, I. *Anal. Chem.* **1967**, *39*, 1514−1527.

(4) (a) Delahay, P.; Trachtenberg, I. *J. Am. Chem. Soc.* **1957**, *79*, 2355−2362. (b) Mohilner, D. M. In *Electroanalytical Chemistry*; Bard, A. J., Ed; Marcell Dekker: New York, 1966; pp 377−409.

(5) (a) Travis, E. R.; Wang, Y. M.; Michael, D. J.; Caron, M. G.; Wightman, R. M. *Proc. Natl. Acad. Sci.* **2000**, *97*, 162−167. (b) Logman, M. J.; Budygin, E. A.; Gainetdinov, R. R.; Wightman, R. M. *J. Neurosci. Methods* **2000**, *95*, 95−102.

(6) Adams, R. N. *Prog. Neurobiol.* **1990**, *35*, 297−311.

(7) Garris, P. A.; Kilpatrick, M.; Bunin, M. A.; Michael, D.; Walker, Q. D.; Wightman, R. M. *Nature* **1999**, *398*, 67−69.

10.1021/ac000849y CCC: $19.00
Published on Web 11/17/2000

including net DA concentration released per action potential and the rate of DA uptake into neurons afterward. These events occur on rapid time scales, less than 1 s, and thus, it is important to understand dopamine adsorption/desorption kinetics over these durations. Herein, background-subtracted, high repetition, fast-scan cyclic voltammetry (FSCV)[9] is used to investigate DA and DOQ adsorption/desorption kinetics at carbon-fiber microelectrodes.

EXPERIMENTAL SECTION

Chemicals. Aqueous solutions were prepared using water from a Megapure system (Corning model D2) which was subsequently distilled before use (Corning MegaPure MP-3A). Dopamine, NaCl, HEPES, and $CaCl_2$ were obtained from Sigma-Aldrich. All solutions were adjusted to pH = 7.4 using NaOH (Aldrich). Norit A activated carbon (ICN) was used to purify reagent grade 2-propanol (Mallinckrodt).

Flow Injection Apparatus. The experimental setup has been previously described.[10] An electrode was positioned at the outlet of a flow injection apparatus. The apparatus consisted of a six-port HPLC loop injector that was mounted on a two-position actuator (Rheodyne model 5041 valve and 5701 actuator) which was used with a 12-V DC solenoid valve kit (Rheodyne) to precisely introduce DA to the surface of the electrode. Solvent flow was driven by gravity through the valve and into the electrochemical cell.

Electrodes. Glass-encased carbon fiber T650 and P55 (Thornel, Amoco Corp., Greenville, SC) microelectrodes were constructed as previously described.[11] Prior to use, the microelectrodes were polished on a diamond-coated polishing wheel (Sutter Instrument Co., Novato, CA). The exposed elliptical carbon surface was soaked in purified 2-propanol (Fisher Scientific) prior to use for electrochemical detection, vide infra. Electrodes were backfilled with a solution of 4 M potassium acetate/0.15 M NaCl to provide electrical connection to an inserted stainless steel wire.

Data Acquisition. The FSCV measurement system has been recently refined to maximize S/N, which is of great importance for electrochemical detection of catecholamine release in vivo.[12] Data acquisition hardware and software (written in LabVIEW) have been previously described.[12a] Computer-generated waveforms were input into a patch clamp integrating amplifier (Axopatch model 200B) for application to the electrochemical cell. A custom built headstage (UNC department of chemistry electronics shop) was used for current transduction for signals which had large currents (0.5 μA), observed often with faster scan rate protocols. Signals were digitally acquired through an acquisition board (model PCI-6110E National Instruments) interfaced to a PC (450 MHz Pentium III Midwest Micro). A timing board (model PC-TIO-10 National Instruments) was used to synchronize flow injection, data acquisition, and waveform application events. Experimental data were imported into Transform (Fortner Software LLC, Sterling, VA) where background subtraction, signal averaging, and digital filtering (nearest 3D neighbor 8 point smooth) were performed.

Table 1. Pretreatment of Carbon-Fiber Microelectrodes

treatment	duration	n	sensitivity (% of control)	S/N (% of control)
P55 Disks				
AC:IPA sonicate	10 min	16	640 ± 110	110 ± 20
AC:IPA stir	10 min	8	1400 ± 500	110 ± 4
AC:IPA sonicate	15 s	8	140 ± 10	100 ± 20
AC:IPA soak	10 min	4	150 ± 20	180 ± 40[a]
purified IPA soak	10 min	8	170 ± 20	180 ± 40[a]
purified IPA soak	overnight	14	240 ± 40	250 ± 30[a]
T650 Cylinders				
purified IPA soak	10 min	8	260 ± 50	330 ± 80[a]
purified IPA soak	overnight	6	300 ± 50	380 ± 100[a]

[a] S/N is statistically different from the pretreatment value using a paired t-test at a 95% confidence level. Purified IPA was prepared by adding 0.1 g/mL AC overnight and then filtering prior to use.

Biological Experiments. Brain slices containing the caudate-putamen were taken from freshly sacrificed mice (C-57 black, Jackson Laboratories). The mice were decapitated and the skull was removed. After extraction of the brain, 400-μm slices were made with a vibrating microtome (World Precision Instruments) and stored in buffer until experiments were performed.[13] Electrodes were positioned in the brain slice using micropositioners (Narishige).

For in vivo experiments, male Sprague−Dawley rats (Charles River Laboratories) were anesthetized with 50% w/w urethane in saline solution (0.3 mL/100 g rat weight) and mounted in a stereotaxic frame. Holes were drilled in the skull to allow access to the caudate-putamen for the cylinder microelectrode placement (stereotaxic coordinates: AP, 1.2; ML, +2.0; DV, −4.5) and to the ventral tegmental region for stimulator placement (stereotaxic coordinates: AP, −5.6; ML, +1.0; DV, −7.5).[14]

RESULTS AND DISCUSSION

Microelectrode Pretreatment. McCreery et al. have reported that increased heterogeneous electron transfer (ET) kinetics correlate with strength of adsorption for DA at glassy carbon (GC).[1,15] Increased ET kinetics have been observed by soaking GC electrodes in 2-propanol (IPA) containing activated carbon (AC) with stirring or sonication.[1] Because stronger adsorption correlates with increased sensitivity, the effects of these pretreatments were investigated at carbon fibers. Electrode sensitivity to DA was evaluated by FSCV before and after treatment. The traditional pretreatment in this laboratory (control in Table 1) is to soak electrodes in reagent grade IPA for 10 min.[11a] Soaking P55 disk microelectrodes in IPA containing AC with stirring or sonication showed marked increases in sensitivity in comparison

(8) (a) Imperato, A.; Di Chiara, G. *J. Pharmacol. Exp. Ther.* **1986**, *239*, 219−239. (b) Jones, S. R.; Garris, P. A.; Wightman, R. M. *J. Pharmacol. Exp. Ther.* **1995**, *274*, 396−403.

(9) Howell, J. O.; Kuhr, W. G.; Ensman, R. E.; Wightman, R. M. *J. Electroanal. Chem.* **1986**, *209*, 77−91.

(10) Kristensen, E. W.; Wilson, R. L.; Wightman, R. M. *Anal. Chem.* **1986**, *58*, 986−988.

(11) (a) Kawagoe, K. T.; Zimmerman, J. B.; Wightman, R. M. *J. Neurosci. Methods* **1993**, *48*, 225−240. (b) Hochstetler, S. E.; Puopolo, M.; Gustincich, S.; Raviola, E.; Wightman, R. M. *Anal. Chem.* **2000**, *72*, 489−496.

(12) (a) Michael, D. J.; Joseph, J. D.; Kilpatrick, M. R.; Travis, E. R.; Wightman, R. M. *Anal. Chem.* **1999**, *71*, 3941−3947. (b) Michael, D. J.; Travis, E. R.; Wightman, R. M. *Anal. Chem.* **1998**, *70*, 586A-592A.

(13) (a) Dingledine, R.; Dodd, J.; Kelly, J. S. *J. Neurosci. Methods* **1980**, *2*, 3323−3362. (b) Kelly, R. S.; Wightman, R. M. *Brain Res.* **1987**, *423*, 79−87.

(14) Wightman, R. M.; Amatore, C. M.; Engstrom, R. C.; Hale, P. D.; Kristensen, E. W.; Kuhr, W. G.; May, L. J. *Neurosci.* **1988**, *25*, 513−523.

(15) DuVall, S. H.; McCreery, R. L. *Anal. Chem.* **1999**, *71*, 4594−4602.

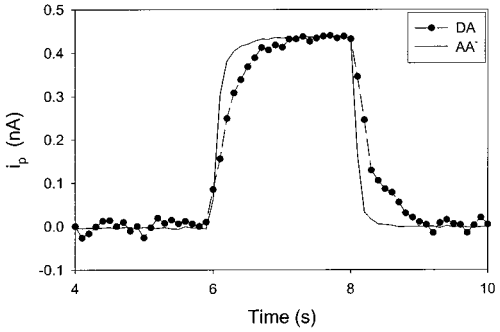

Figure 1. Dynamic response of the oxidative peak current (i_p), measured at a T650 disk microelectrode, to 2.0-s injections of AA^- and DA. A 300 V/s 10 Hz waveform is applied. Solution conditions are 100 μM AA^- or 2.5 μM DA in (mM): NaCl (150), HEPES (20), and $CaCl_2$ (1.2) brought to pH = 7.4 by adding NaOH.

to the traditional pretreatment; however, electrode noise also increased (Table 1). Scanning electron micrographs of electrodes after sonicating (data not shown) showed large increases in surface roughness, which likely result in the lack of increase in S/N. In contrast, soaking P55 disk microelectrodes in AC:IPA solutions without agitation increased sensitivity without increasing noise (Table 1). IPA was purified by pretreating with 0.1 g/mL AC and then filtering to remove the AC. Soaking P55 disk and T650 cylinder microelectrodes in this purified IPA also showed increases in S/N that appeared to improve with soak duration. The largest improvement was observed for cylinders, ~400%. All experiments described hereafter were performed on microelectrodes that were soaked a minimum of 20 min in purified IPA.

Response of Microelectrodes in the Flow Cell. In the experiments described herein, electrodes were positioned at the outlet of a flow cell where a bolus of electroactive species could be precisely introduced and removed from the electrode surface. The electrode potential was held at ~−0.4 V vs Ag/AgCl and ramped to a peak potential of ~1.0 V. The potential was then ramped back to the holding potential. This process was repeated at varying frequencies. The average current from a potential window centered around the oxidative peak current (i_p) for the electroactive species was then chosen and plotted as a function of scan number (duration of the experiment).

To demonstrate that the flow cell is capable of generating rapid concentration changes, the electrochemical responses at a T650 microelectrode disk were compared during injections of DA and a species that does not adsorb (ascorbate, AA^-). Figure 1 shows i_p as a function of time for 2.0-s injections of AA^- and DA. AA^- exhibits a relatively square response as that expected for a bolus injection to the electrode surface. Comparatively, DA exhibits a much slower temporal response under identical conditions. The slower response is attributed to dopamine and dopamine-*o*-quinone adsorption and desorption kinetics because mass transport for it and ascorbate are governed by the same process.

Evidence for Adsorption. Polished carbon surfaces have a significant amount of oxides.[16] These sites are favorable for adsorption of cationic species, such as DA, whose amine side chain is protonated at physiological pH. Furthermore, the polished surfaces on our electrodes are rough, having large step-edge

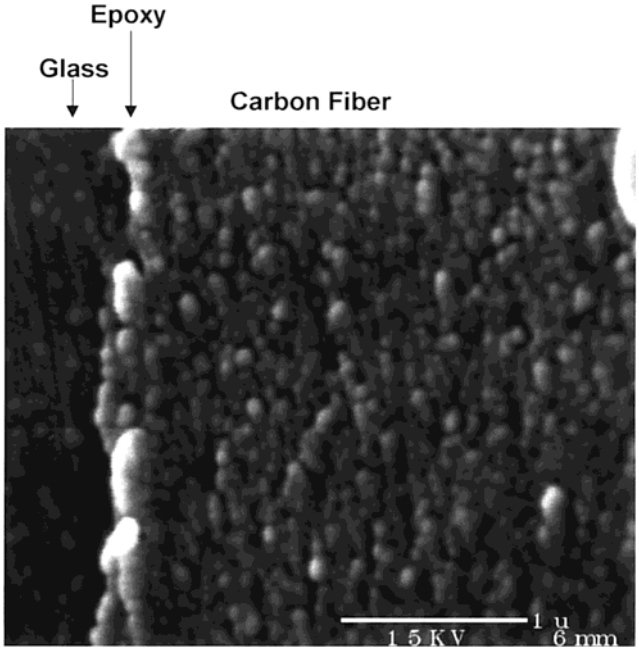

Figure 2. SEM image of a polished P55 disk microelectrode. The fiber was polished and soaked in purified IPA overnight prior to imaging. Scale bar = 1.0 μm.

features across the entire fiber cross-section. An SEM of a P55 disk is shown in Figure 2. This electrode was polished on a diamond-coated polishing wheel and allowed to soak overnight in purified IPA before being imaged in ultrahigh vacuum. Step edges are favorable for adsorption and may also influence the process of DA electrooxidation.[17]

In cyclic voltammetry, the current that is due to double-layer charging is proportional to the electrode area. Because of the rough surface, illustrated in Figure 2, this contributes to large background currents that increase linearly with the voltammetric scan rate. The faradaic current due to electrooxidation or reduction of a nonadsorbing species (e.g., AA^- in Figure 1) is proportional to the square root of the scan rate. Often this results in the faradaic signal being lost in the background as the scan rate is increased. In contrast, the faradaic current due to electrooxidation or reduction of an adsorbed species is proportional to the scan rate.

DA is oxidized in a two-electron oxidation ($E^{o\prime}$ = 0.11 vs SCE),[18]

$$DA \rightarrow DOQ + 2e^- + 2H^+$$

where DOQ is the *o*-quinone form of DA. In Figure 3, the peak current (i_p) due to electrooxidation of DA at a P55 disk is plotted as a function of scan rate. The response is linear, which indicates that DA adsorbs to the electrode. The symmetrical shape of the voltammogram waves at 300 V/s and 2000 V/s is also consistent with adsorption of DA (Figure 3).[2,19] Similar responses are observed at T650 disk and cylindrical microelectrodes (data not shown).

(16) McCreery, R. L. In *Electroanalytical Chemistry*; Bard, A. J., Ed.; Marcell Dekker: New York, 1991; Vol. 17, p 363.

(17) Niemantsverdriet, J. W. *Spectroscopy in Catalysis*; VCH Publishers: New York, 1995; pp 1−4.

(18) Tse, D. C. S.; McCreery, R. L.; Adams, R. N. *J. Med. Chem.* **1976**, *19*, 37−40.

(19) Laviron, E. *J. Electroanal. Chem.* **1974**, *52*, 395−402.

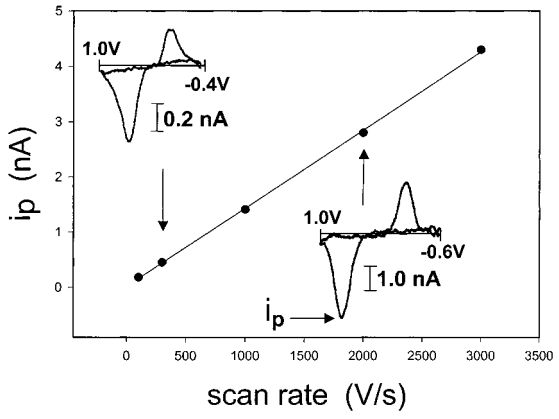

Figure 3. Peak faradaic current (i_p) observed on the oxidative voltammetric wave for DA at a P55 disk microelectrode as a function of scan rate. The electrode is placed at the outlet of a flow injection apparatus, and voltammograms are recorded at 10 Hz. Voltammograms taken before DA exposure are subtracted from those obtained during the presence of DA. The electrode is exposed long enough to reach a steady-state peak current (~2.0 s). The voltammograms on the inset represent those obtained at 300 V/s and 2000 V/s. Each data point represents the average of three measurements. The size of each point represents ±1 SEM. Solution conditions are 2.5 μM DA in the same buffer system as that for Figure 1.

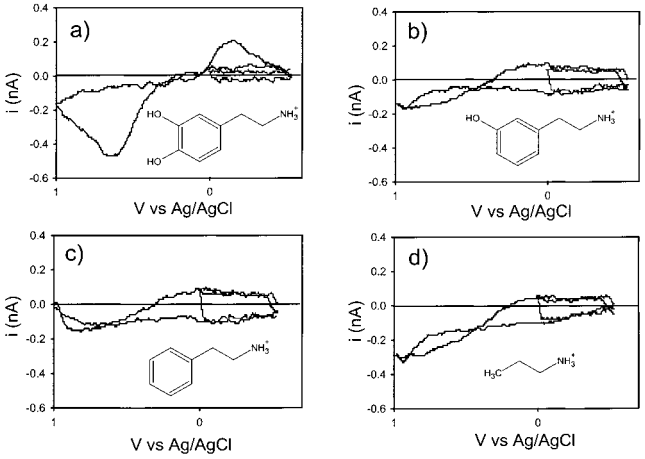

Figure 4. Background-subtracted cyclic voltammograms of (a) dopamine, (b) tyramine, (c) phenethylamine, and (d) propylamine at a T650 disk microelectrode. Two waveforms are applied for detection of each molecule. First, a waveform capable of electrooxidizing catecholamines, −0.4 to 1.0 to −0.4 V vs Ag/AgCl, is applied. Second, a waveform which should not produce faradaic current due to catecholamine oxidation, −0.4 to 0.0 to −0.4 V vs Ag/AgCl, is applied. The voltammetric waveforms have a scan rate of 300 V/s and are taken at 10 Hz. The concentration of each molecule is 2.5 μM in the same buffer system as that for Figure 1.

The amine side chain of dopamine is protonated at physiological pH. Other alkylamines were chosen to determine whether this functionality was responsible for adsorption to the electrode surfaces. In Figure 4, background-subtracted cyclic voltammograms (CVs) at a T650 disk microelectrode are shown for dopamine, tyramine, phenethylamine, and propylamine in parts a, b, c, and d, respectively. Two CVs are shown in each plot. The first uses a waveform starting at −0.4 V, going to 1.0 V, and returning to −0.4 V. This waveform is sufficient to oxidize catechol functionalities. The second waveform begins at −0.4 V, ramps to 0.0 V, and returns to −0.4 V. This background-subtracted voltammogram, hereafter referred to as "short CV", should have no faradaic curren due to electrooxidation, and any changes from baseline should be due solely to alterations in double-layer structure, that is, adsorption. In Figure 4a, the short CV of DA exhibits a measurable decrease in background current, evidenced by the positive deflection in the first half (oxidative) of the background-subtracted cyclic voltammogram. This suggests that adsorption is occurring. This effect is also observed with the other three alkylamines (parts b, c, and d), which strongly suggests that it is the amine functionality that is involved in the adsorption at the carbon surface. Similar results are observed at P55 disks and T650 cylinders (data not shown).

The left plot in Figure 5 shows i_p for various DA concentrations (recorded after 2-s exposures in the flow cell) at both P55 and T650 disks. The i_p is proportional to the total charge under the oxidative voltammetric peak (Q) which is a measure of the coverage of DA (Γ_{DA}) on the electrode surface ($i_p \propto Q/nFA = \Gamma_{DA}$).[2] The curves appear not to exhibit limiting DA coverage at high DA solution concentrations. Comparison of the cyclic voltammmograms that are observed at lower DA concentration (2.5 μM) to those that are observed at higher concentration (400 μM) indicates a diffusional component at higher concentrations (Figure 5). At 400 μM, the oxidative current decays toward baseline more slowly than at lower concentrations, which is consistent with diffusional mass transport.

Simulations were performed using DigiSim to predict the diffusion-controlled response of the electrodes (Figure 5, dashed lines). These data were digitally subtracted from that realized in experiment to obtain voltammetrically measured isotherms. Fitting a Langmuir isotherm to the corrected data (solid lines, right plot) shows good agreement between experiment and theory. Thus, for low concentrations of DA (<25 μM), adsorption is the primary contribution to the analytical signal. The Langmuir isotherm predicts that the slope at low Γ_{DA} is proportional to the concentration of DA in solution. In Figure 5 this slope is calculated to be $\sim 3 \times 10^{-3}$ cm for both the P55 and T650 disks. A limiting coverage of $\sim 10^{-10}$ mol/cm^2 is obtained for both electrodes. This is similar to that measured for a monolayer coverage of amine side-chain containing phenyl compounds ($\Gamma^{sat} = 3 \times 10^{-10}$ mol/cm^2 for platinum electrodes).[20] However, such agreement may be fortuitous because our calculation does not account for the surface roughness of the carbon electrode.

Effect of Repetition Rates. Figure 6 shows the temporal responses observed at P55 (a) and T650 (b) disk electrodes to 0.5-s exposures of 2.5 μM DA in the flow cell. Cyclic voltammetry was applied at a scan rate of 2000 V/s at various repetition frequencies. The peak voltammetric currents (i_p) were measured and converted to the coverage of DA, Γ_{DA}, vide supra. Two interesting features are apparent in these data: First, with higher repetition rates, the maximal Γ_{DA} diminishes. This indicates that the amount of adsorbed DA is lowered with shorter intervals between scans. Second, the rate at which the steady-state Γ_{DA} is achieved is more rapid with increasing repetition rates. At the maximal repetition rate employed, 240 Hz, the curves in Figure 6 approach the rectangular shape that the solution concentration has in the exit of the flow cell,which indicates that diffusion control is approached.

(20) Soriaga, M. P.; Hubbard, A. T. *J. Am. Chem. Soc.* **1982**, *104*, 2735−2742.

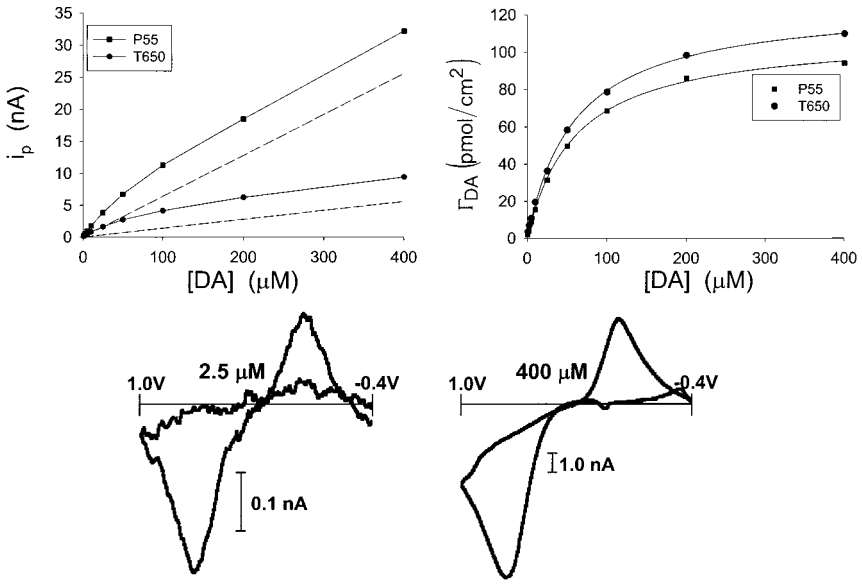

Figure 5. Left plot: Voltammetrically measured oxidative peak currents for DA at T650 (●) and P55 (■) disk microelectrodes. The points shown are averages of three measurements and their size represents ±1 SEM. The dashed lines represent simulated diffusion-controlled responses. Right plot: Fits of the Langmuir isotherm to the diffusion-corrected experimental data. The voltammograms shown at the bottom are taken from the data reported for the T650 electrode. Solution conditions are identical to those in Figure 1.

DA adsorption was also examined with high-speed chronoamperometry.[21] To approximate a step, the applied potential was ramped at 16 000 V/s and then held at a potential sufficient to oxidize DA_{ads} (+0.5 V vs Ag/AgCl) or reduce DOQ_{ads} (−0.3 V vs Ag/AgCl). Steps had a repetition rate of 10 Hz. The total time for the forward step was 200 μs (Figure 7). The background-subtracted current observed at a T650 disk shows two peaks of alternate sign corresponding to electrochemical detection of adsorbed species. The dynamic response of Γ_{DA} measured from repeated steps during a 1.75-s injection of 2.5 μM DA is shown in Figure 7.

Kinetic Model of the Data. The voltammetric results indicate that increased sensitivity for DA can be achieved by scanning the electrode faster (Figure 3). In contrast, as shown in Figure 6, the rate at which the electrode achieves a steady-state response can be accelerated by increasing the repetition rate of applied voltammetric waveforms. Unfortunately, high CV repetition rates reduce the sensitivity gained by faster electrode scanning. A kinetic model is now described that explains the observed behavior.

In describing the dynamic response of the faradaic current at an electrode positioned at the outlet of a flow cell, it is necessary to model DA and DOQ adsorption and desorption

$$DA_{soln} \underset{k_{-1}}{\overset{k_1}{\rightleftharpoons}} DA_{ads} \overset{-2e}{\rightleftharpoons} DOQ_{ads} \underset{k_2}{\overset{k_{-2}}{\rightleftharpoons}} DOQ_{soln} \qquad (1)$$

In eq 1, DA_{soln} and DOQ_{soln} are the solution-based forms of the catechol and o-quinone, respectively, and DA_{ads} and DOQ_{ads} are the adsorbed species on the electrode surface. The injection into the flow cell is considered to occur instantaneously, as depicted in Figure 6 (top). Thus, DA_{soln} is either 0 or some finite concentration. The value of DOQ_{soln} is normally 0, but is considered to be equal to the original concentration of DA_{soln} during the portion of the voltage sweep when oxidation occurs. Of course, this is an approximation and is true only for the thin region of the solution directly adjacent to the electrode.

In eq 1, the rates of adsorption and desorption of DA are assumed to be first order. Thus, the rate equation may be expressed as

$$\frac{d\Gamma_{DA}}{dt} = k_1[DA] - k_{-1}\Gamma_{DA} \qquad (2)$$

Similarly, the rates of adsorption and desorption of DOQ are assumed to be first order

$$\frac{d\Gamma_{DOQ}}{dt} = k_2[DOQ] - k_{-2}\Gamma_{DOQ} \qquad (3)$$

Equation 2 describes the behavior at the rest potential and at the initial part of the voltage scan, whereas eq 3 describes processes occurring at potentials sufficient to oxidize DA during the cyclic voltammetric scan. A typical waveform ($E(V)$) is shown in the top portion of Figure 6. The processes occurring during the time period denoted by τ are described by eq 2, whereas those occurring during the time period denoted by t_s are described by eq 3. We have assumed that DOQ_{ads} is present for 60% of the voltammetric scan. For example, for 300 V/s and potential limits of −0.4 and 1.0 V, the duration of the scan is about 10 ms. Therefore, t_s is equal to 6 ms (Figure 6). The value of τ is determined by both the voltammetric scan and the repetition rate. Continuing with the previous example, with 10 Hz measurements, τ is equal to 94 ms (4 ms from the scan and 90 ms from the repetition rate). In chronoamperometry, these times are more precisely defined (Figure 7). The model iterates between these two time domains, calculating Γ_{DA} for each cycle. A hypothetical electrode response showing the dynamics of DA coverage (Γ_{DA}) is shown in Figure 6.

(21) (a) Forster, R. J. *Langmuir* **1995**, *11*, 2247−2255. (b) Forster, R. J. *Anal. Chem.* **1996**, *68*, 3143−3150.

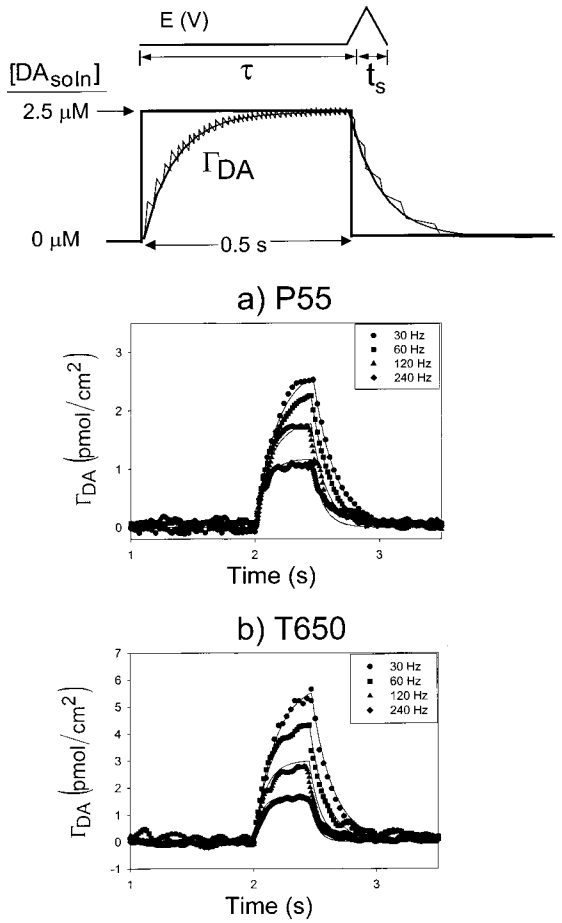

Figure 6. Top: Kinetic model describing DA adsorption/desorption kinetics. Two time domains are defined over a typical waveform, $E(V)$ according to whether DA (τ) or DOQ (t_s) is present on the electrode surface. DA is introduced as a plug injection for a specified duration. The slow response of the electrode is shown as the coverage of DA on the electrode surface, Γ_{DA}. Individual iterations of the model are sketched over the electrode response. Bottom: Γ_{DA} temporal responses at (a) P55 and (b) T650 disk microelectrodes to 0.5-s injections of DA in the flow cell as a function of voltammetric repetition rate. The voltammetric scan rate was 2000 V/s for all profiles. The solid lines represent the best fits of eqs 6 and 10 to the experimental data that was obtained by minimizing the squares of the residuals. Fitted parameters: (a) $k_1 = k_2 = 7.7 \times 10^{-3}$ cm/s; $k_{-1} = 5.0$ s^{-1}, and $k_{-2} = 35$ s^{-1}; (b) $k_1 = k_2 = 1.4 \times 10^{-2}$ cm/s; $k_{-1} = 4.2$ s^{-1}; $k_{-2} = 40$ s^{-1}. Solution conditions were 2.5 μM DA in pH = 7.4 buffer. Data were filtered in Transform to eliminate high-frequency noise components to the observed signal. This did not distort the temporal response.

Integration of eqs 2 and 3 using the boundary conditions that $\Gamma_{DA} = \Gamma^{\circ}_{DA}$ and $\Gamma_{DOQ} = \Gamma^{\circ}_{DOQ}$ at $t = 0$ yields

$$\Gamma_{DA} = \left(\frac{k_1[DA]}{k_{-1}}\right) + \left(\Gamma^{\circ}_{DA} - \frac{k_1[DA]}{k_{-1}}\right)(e^{-(k_{-1}\tau)}) \qquad (4)$$

and

$$\Gamma_{DOQ} = \left(\frac{k_2[DOQ]}{k_{-2}}\right) + \left(\Gamma^{\circ}_{DOQ} - \frac{k_2[DOQ]}{k_{-2}}\right)(e^{-(k_{-2}t_s)}) \qquad (5)$$

It is important to note that the initial coverages for each successive iteration (Γ°_{DA} and Γ°_{DOQ}) are determined by the final coverage of the previous step. Thus, at each application of a potential change, $\Gamma^{\circ}_{DOQ} = \Gamma_{DA}$ at the beginning of t_s and $\Gamma^{\circ}_{DA} = \Gamma_{DOQ}$ at the beginning of τ. The succession of iterations can be written in the form of a sum

$$\Gamma_{DA} = \left[\frac{k_1[DA]}{k_{-1}}(e^{k_{-1}\tau} - 1) + \frac{k_2[DOQ]}{k_{-2}}(e^{k_{-2}t_s} - 1)(e^{k_{-1}\tau})\right] \times \sum_{n=1}^{m} e^{-n[k_{-1}\tau + k_{-2}t_s]} \qquad (6)$$

Each value of n corresponds to one complete cycle ($\tau + t_s$). The sequential steps, each representing a successive cycle (value of m), model the electrode response and lead to the smooth line in Figure 6.

For m approaching infinity, the geometric series in eq 6 has a well-defined convergence point, eq 7[22]

$$\Gamma^{ss}_{DA} = \frac{\frac{k_1[DA]}{k_{-1}}e^{-k_{-2}t_s}(1 - e^{-k_{-1}\tau}) + \frac{k_2[DOQ]}{k_{-2}}(1 - e^{-k_{-2}t_s})}{1 - e^{-(k_{-1}\tau + k_{-2}t_s)}} \qquad (7)$$

where Γ^{ss}_{DA} is the steady-state coverage of DA on the electrode.

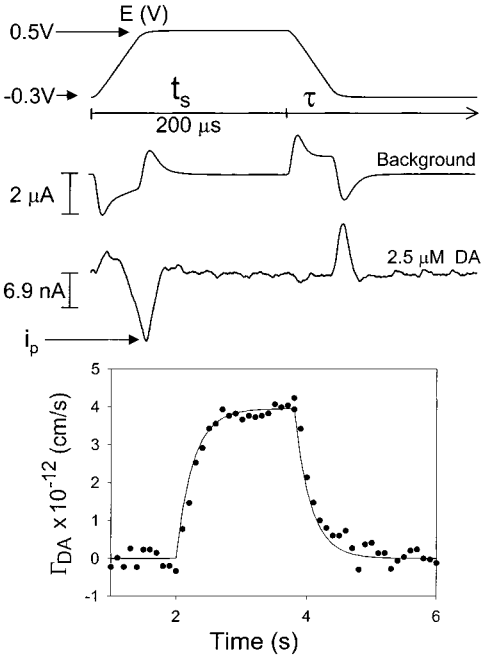

Figure 7. High repetition chronoamperometry. The electrode potential ($E(V)$) is ramped at 16 000 V/s to a potential positive of $E^{\circ\prime}$ for the DA/DOQ redox reaction (+0.5 V vs Ag/AgCl) such that only DOQ is present on the electrode surface (t_s). The electrode is then ramped back to a holding potential (−0.3 V vs Ag/AgCl) at 16 000 V/s such that only DA is present at the electrode surface (τ) until the next waveform is applied (10 Hz). The nonfaradaic current that was observed at the electrode is shown (background). This is subtracted from the electrode response when DA is present to obtain the current solely due to DA and DOQ detection (2.5 μM DA). Lower plot: Γ_{DA} temporal response at a T650 disk microelectrode to a 1.75-s injection of 2.5 μM DA in the flow cell. The solid line shows the best fit of eqs 6 and 10 to the experimental data. Fitted parameters: $k_1 = k_2 = 6.2 \times 10^{-3}$ cm/s; $k_{-1} = 4.0$ s^{-1} and $k_{-2} = 30$ s^{-1}. The data were filtered to remove high-frequency noise. This process did not perturb the temporal response.

Following the injection, $[DA_{soln}] = 0$, and the electrode response slowly approaches that for $\Gamma_{DA} = 0$. Here, eqs 4 and 5 become

$$\Gamma_{DA} = \Gamma^{F}_{DA}(e^{-(k_{-1}\tau)}) \quad (8)$$

and

$$\Gamma_{DOQ} = \Gamma'_{DOQ}(e^{-(k_{-2}t_s)}) \quad (9)$$

where Γ^{F}_{DA} is the final coverage of DA at the end of the injection and Γ'_{DOQ} is the initial concentration of DOQ on the first scan after $DA_{soln} = 0$. Subsequent iterations use initial concentrations corresponding to the final concentrations for the previous step. Thus, combining eqs 8 and 9 shows that Γ_{DA} decreases as a function of the two times of the cyclic voltammogram, eq 10

$$\Gamma_{DA} = \Gamma^{F}_{DA} e^{-m[k_{-1}\tau + k_{-2}t_s]} \quad (10)$$

where m in this equation is the cycle number since the removal of DA from the electrode vicinity.

Kinetics at Disk Microelectrodes. In Figure 6, the solid lines on each plot represent the best fit of the model (eqs 6 and 10) to the data. The model predicts that by decreasing the amount of time when k_1 and k_{-1} are operant (increasing CV repetition rate), the steady-state DA coverage will be reduced. In addition, the model predicts that steady-state Γ_{DA} is reached much faster by performing voltammetry at high repetition rates. These predicted behaviors follow those that are observed in experiments. The finding that steady-state is reached faster at, for example, 240 Hz, is a result of τ and t_s approaching equality, that is, minimal time where k_1 and k_{-1} operate, which leads to lower equilibrium Γ_{DA}.

The model was fit to the data as shown in Figure 6. The model requires estimation of four rate constants. The values of k_{-1} and k_{-2} can be estimated independently of the others during the time when DA is removed from the electrode surface (eq 10). Because the amplitude decreases with increasing repetition rate, DOQ must adsorb more weakly than DA. Therefore, to simplify the analysis, the values of k_2 and k_1 were made equal, and the fit only involved adjusting values of k_1, k_{-1}, and k_{-2}. The importance of the amine in adsorption provides support for this simplification.

In Table 2, the rate constants used to describe DA and DOQ adsorption/desorption kinetics at disk electrodes are shown for voltammetric scan rates of 300 V/s and 2000 V/s. One value of k_1 (and thus, k_2) could describe results at both scan rates (Table 2). However, they were lower at P55 disks, which indicates greater adsorption at T650 disks. The greater equilibrium Γ_{DA} at T650 disks is consistent with the voltammetrically measured isotherms (Figure 5). From the Langmuir isotherms in Figure 5, the equilibrium constant (k_1/k_{-1}) relating DA_{soln} to Γ_{DA} at low DA_{soln} is calculated to be $\sim 3 \times 10^{-3}$ cm. Inspection of Table 2 shows $k_1/k_{-1} = 1.4 \times 10^{-3}$ cm and 2.6×10^{-3} cm for P55 and T650 disks, respectively, which is in agreement with what was predicted. The rate constants for desorption for DA (k_{-1}) and DOQ (k_{-2}) were unaffected by changes in the voltammetric scan rate or fiber type.

Table 2. Fitted Model Parameters Describing DA and DOQ Adsorption/Desorption Kinetics at P55 and T650 Disk Microelectrodes[a]

	$k_1 \times 10^3$ (cm/s)	k_{-1} (s^{-1})	k_{-2} (s^{-1})	$e^{-(k_{-2}t_s)}$
P55 (300 V/s)	8.6 ± 1.9	5.5 ± 1.5	23 ± 9	0.87 ± 0.04
P55 (2000 V/s)	7.7 ± 2.8	5.9 ± 2.0	38 ± 16	0.97 ± 0.01
mean	8.1	5.7	31	
T650 (300 V/s)	12 ± 3	5.0 ± 1.0	22 ± 6	0.88 ± 0.03
T650 (2000 V/s)	13 ± 5	5.0 ± 1.0	47 ± 9	0.96 ± 0.01
mean	13	5.0	35	

[a] Entries are averages ±1 SEM ($n = 5$). The value for k_2 was set equal to k_1 in all simulations.

The value of k_{-2} is larger than k_{-1}, which is consistent with less adsorption of DOQ than DA. The rate constants obtained from chronoamperometric data (Figure 7) are in agreement with the voltammetric results.

The model does not exactly predict the voltammetric response, however. The last column in Table 2 gives the relative amount of DOQ to DA predicted by eq 9. Thus, i_p^{red} should be ~90−97% of the oxidative peak current (i_p), whereas the voltammetry shows $i_p^{red} = (0.6)i_p$ (e.g., Figure 3). This discrepancy could be due to three effects. First, a percentage of DOQ could instantly desorb after production. If this is true, then DA readsorption at these sites must be fast enough such that all sites occupied on the previous waveform application are again present for the next waveform application event. If this were not true, the model would not fit the oxidative data as shown in Figure 6. Second, the discrepancy could have a heterogeneous electron-transfer origin. The electrooxidation of DA on carbon fibers at pH = 7.4 proceeds by 2 individual H^+, e^- steps.[23] Thus, the second 1 e^- reduction may be rate-limited by the concentration of H^+ at the electrode surface. The second 1 e^- reduction must occur between scans for the model to fit the data as shown in Figure 6. In fact, continuing to record current between waveforms often shows continued reductive current (data not shown). Experiments at lower solution pH values are complicated by the fact that the surface oxides on carbon protonate[24] and the cyclic voltammograms of DA become more diffusion-controlled. However, at pH = 3, $i_p^{red} = (0.9)i_p$ (data not shown). Quantitative assessments of this are impractical because of the changes in surface chemistry. Third, because the waveform has a holding potential of −0.4 V, there may be electrostatic contributions to the oxidative current for the cationic species DA. Applying a waveform that holds the electrode at 0 V vs Ag/AgCl between scans lowers the amount adsorbed and shows $i_p^{red} = (0.75)i_p$. Thus, electrostatic interactions may contribute to the observed adsorption and its discrepancy with the model. The disagreement between the data and the model may well be a combination of all of these factors.

Brain Slice and In Vivo Experiments. Rapid response times such as those shown in Figure 6 are crucial when measuring neurotransmission kinetics in biological systems. To improve S/N

(22) Purcell, E. J.; Varberg, D. *Calculus with Analytic Geometry*; Prentice Hall, Inc: Upper Saddle River, NJ, 1987; p 473.

(23) Kawagoe, K. T.; Garris, P. A.; Wightman, R. M. *J. Electroanal. Chem.* **1993**, *359*, 193−207.

(24) Runnels, P. L.; Joseph, J. D.; Logman, M. J.; Wightman, R. M. *Anal. Chem.* **1999**, *71*, 2782−2789.

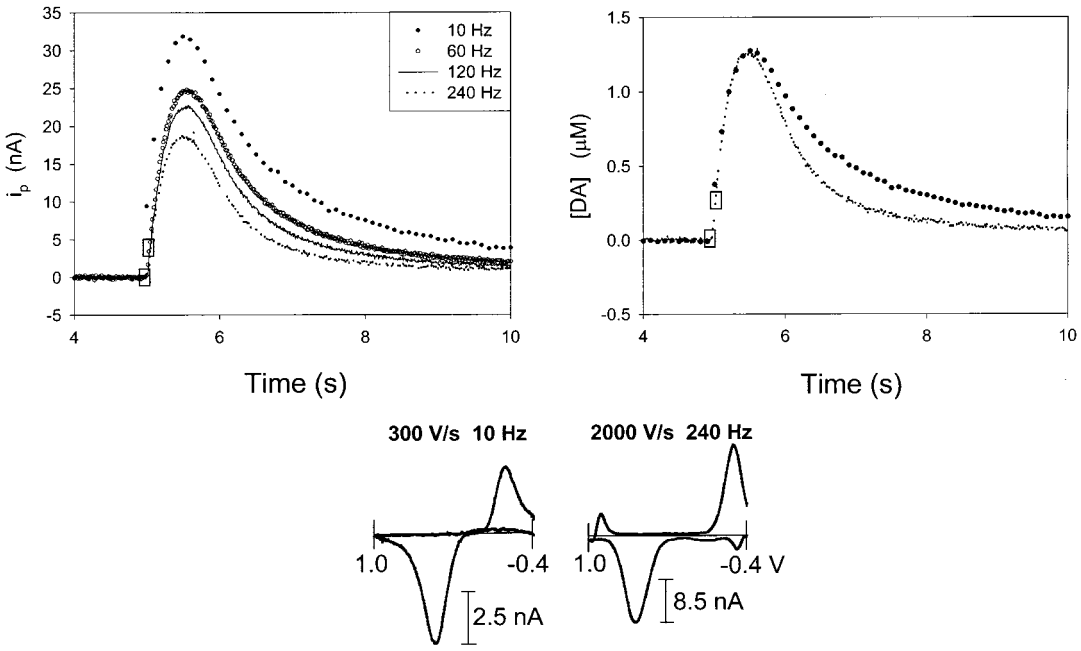

Figure 8. Voltammetric oxidative peak (i_p) temporal profiles at a 75-μm cylinder microelectrode placed in the caudate region of a mouse brain slice. A 300-μA biphasic pulse is applied for 10 ms using a stimulating electrode positioned approximately 100 μm from the cylinder electrode. The beginning and ending of the pulse is marked by the boxes. Scan rates of 2000 V/s were used for electrochemical detection of DA at CV repetition rates of 10 (●), 60 (○), 120 (−), and 240 (- - -) Hz. Each profile shown is the average of three scans taken under identical experimental conditions. Left panel: peak cyclic currents (i_p) recorded at different repetition rates. Right panel: data from the left panel was converted to concentration on the basis of precalibration factors. The cyclic voltammograms (lower panels) are taken from the temporal profiles at their maximal values (300 V/s 10 Hz profile not shown). S/N was identical using both experimental protocols. Data were filtered to eliminate high-frequency noise components to the observed signal. This did not distort the temporal response.

by increasing the electrode area, microelectrode cylinders are frequently used in these experiments. Cylinders exhibit temporal profiles in the flow cell that are similar to those for the disks shown in Figure 6. However, they exhibit tailing after termination of the DA pulse, which implies more complicated overall processes than predicted by the model presented herein. The tailing was considered a secondary effect because the primary observations at disks are also observed at cylindrical electrodes.

The effects of increasing CV frequency on measured DA uptake kinetics in the caudate region of a brain slice were investigated. Release of DA was achieved electrically by applying a single 300-μA pulse to a stainless steel electrode positioned ~100 μm from a cylinder electrode. The left plot of Figure 8 shows the electrode response at various CV repetition frequencies corresponding to oxidation of DA after a 10-ms stimulation has been applied. The right plot illustrates the differences in peak shapes when the 240 and 10 Hz responses are scaled to their respective concentrations. As expected, the electrode precalibrated responses at differing CV frequencies leads to different conversion factors (nA/μM) at 10 and 240 Hz. However, when the tissue results are converted to concentration with these factors, the maximal [DA] released is identical. The temporal responses to the appearance of DA, shown by the rising slopes in the right plots of Figure 8, are identical. In contrast, the DA signal after the stimulus decays more rapidly with the 240 Hz repetition rate than with the 10 Hz repetition rate. Michaelis−Menten kinetics have been used to model the rate of uptake of DA from the extracellular space.[25] The maximal rate of uptake, V_{max}, is given by the slope of the curves in Figure 8 immediately after the peak. Its apparent value is greater using the CV repetition rates of 240 Hz. Thus, the rapid repetition rate data more accurately measure the actual uptake kinetics in the caudate by limiting the effects of the slow DA and DOQ adsorption/desorption kinetics. The voltammograms at the bottom of Figure 8 are shown to compare S/N using a traditional measurement protocol, 300 V/s at 10 Hz, to the 2000 V/s at 240 Hz experiments. No significant change in S/N is observed.

The effects of electrode response on CV repetition frequency also were probed in in vivo experiments in anesthetized rats. A cylinder microelectrode was placed in the caudate-putamen to detect DA release evoked by an electrical stimulus similar to the brain slice experiments. Figure 9 shows the voltammetric tip response to a train of 60, 125-μA stimulation pulses. The left plot illustrates the change in temporal profile as a function of voltammetric repetition frequency. Upon converting the current to DA concentration (right plot), a much faster return of DA to baseline is observed after the stimulus using a CV repetition rate of 240 Hz, as compared to 10 Hz. Again, the greater disappearance rate after the stimulus with high repetition rates indicates that the voltammetrically measured maximal rate of DA uptake into the cellular compartments is distorted at low repetition rates by adsorption. The voltammograms at the bottom of Figure 9 are shown to compare S/N using traditional measurements, 300 V/s at 10 Hz, to the 2000 V/s at 240 Hz experiments. S/N decreased by a factor of ~2× in the 2000 V/s at 240 Hz experiments.

CONCLUSIONS

High-repetition fast-scan cyclic voltammetry methodologies have been used to probe sub-second catecholamine adsorption

(25) Wightman, R. M.; Zimmerman, J. B. *Brain Res. Rev.* **1990**, *15*, 135−144.

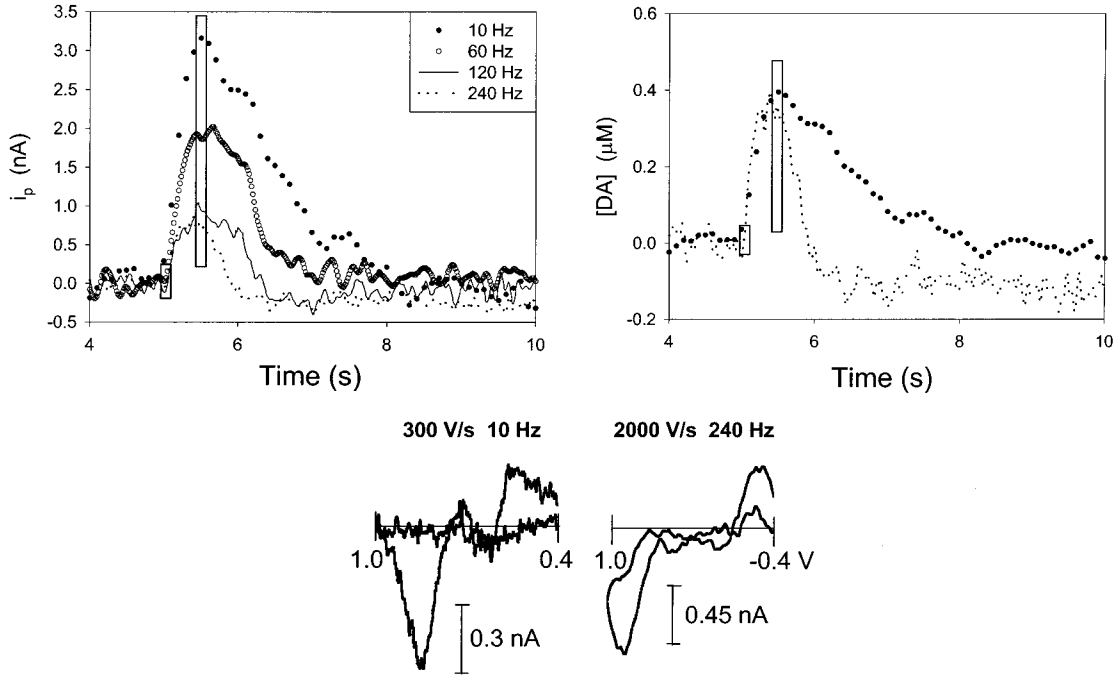

Figure 9. Left panel: i_p responses at a 75-μm cylinder microelectrode placed in the caudate of an anesthetized rat to 60 stimulation pulses having an amplitude of 125 μA. The beginning and ending of the pulse train is denoted by the boxes on the plots. The voltammetric scan rate is 2000 V/s, applied at 10 (●), 60 (○), 120 (−), and 240 (- - -) Hz. Each profile shown is the average of three scans taken under identical experimental conditions. The voltammograms are taken from the temporal profiles at their peak currents (300 V/s 10 Hz profile not shown). S/N was lower by a factor of ~2 for the 2000 V/s, 240 Hz measurements than for measurements recorded at 300 V/s. Data were filtered to reduce high-frequency noise. This did not distort the temporal response. Right panel: data from left panel that was converted to concentration on the basis of precalibration factors.

and desorption at carbon-fiber microelectrodes. The adsorption leads to electrochemical signals of greater amplitude than under diffusion control, but the adsorption kinetics limit the electrode's response to rapid concentration changes. The similarity of several amines in altering the background current (Figure 4) suggests that this portion of the DA molecule is involved in the adsorption. Indeed, dihydroxyphenylacetic acid, a catechol without an aliphatic amine functionality, does not adsorb at carbon fibers to such a high degree.[26] In contrast, at other carbon surfaces, the catechol functionality has been shown to correlate strongly with the degree of observed adsorption.[27] These differences may be due to the different conditions under which adsorption is studied at microelectrodes and electrodes of conventional size. Typically, microelectrodes are used with transient exposure to low concentrations of analytes and with high-speed electrochemical techniques. Electrodes of conventional size have been used with higher concentrations and longer exposure times.

The kinetic model that was developed describes the experimental response of carbon-fiber microelectrodes to DA. Temporally accurate voltammetric responses are most readily obtained with fast scan rates at high frequencies. Like Nafion-coated carbon-fiber electrodes, the bare carbon electrodes exhibit a delayed response to concentrations of species that adsorb at the electrode surface.[28] Understanding this phenomenon is crucial for correctly interpreting transient DA release and uptake in biological systems. Of particular interest is the ability to deconvolute the contributions of adsorption to the overall analytical signal obtained in vivo so that time responses can be corrected, as has been done for data collected at Nafion-coated electrodes.

ACKNOWLEDGMENT

The authors thank Professor Richard McCreery (The Ohio State University) for discussions regarding DA adsorption at glassy carbon. This work was supported by NIH grant number NS 15841.

Received for review July 26, 2000. Accepted October 10, 2000.

AC000849Y

(26) Bauer, J. E.; Kristensen, E. W.; May, L. J.; Wiedemann, D. J.; Wightman, R. M. *Anal. Chem.* **1988**, *245*, 1268−1272.

(27) Allred, C. D.; McCreery, R. L. *Anal. Chem.* **1992**, *64*, 444−448.

(28) Kawagoe, K. T.; Garris, P. A.; Wiedemann, D. J.; Wightman, R. M. *Neuroscience* **1992**, *51*, 55−64.